Proceedings of the 17th World Congress
The International Federation of Automatic Control
Seoul, Korea, July 6-11, 2008

Automated Modelling of Power-Split Hybrid Vehicles

Jinming Liu, Huei Peng

Department of Mechanical Engineering
University of Michigan, Ann Arbor, MI 48109, USA (e-mail: {jinmingl, hpeng}@umich.edu)

Abstract: Hybrid electric vehicles (HEV) represent a promising technology to improve the fuel economy of ground vehicles in the near-term. Among the HEV configurations, the power-split configuration offers superior design and control flexibility and achieves highest overall efficiency. In this paper, a methodology to generate dynamic equations automatically for the power-split hybrid power-train is proposed. The designer only needs to specify the topology of the transmission: how the power sources, vehicle, the planetary gears and clutches are connected to each other. The dynamic model can then be generated automatically through a set of rules. This automated generation process makes it possible for a designer to explore different split hybrid configurations quickly and efficiently.

1. INTRODUCTION

A hybrid electric vehicle (HEV) adds an electric power path to the conventional powertrain, which helps to improve fuel economy by engine right-sizing, load levelling, and re-generative braking. A right-sized engine has higher combustion efficiency, lower heat loss, and reduced peak power. The reduced power is compensated by an electrical machine (or machines) during surged power demand. Compared with internal combustion engines, electric machines provide torque more quickly, especially at low rotational speeds. Therefore, launching performance can be improved, even with reduced rated power. Load levelling can also be achieved by adding the electrical path. With the electric drive assistance, the engine can be controlled to operate in an optimal region regardless of the road load. Finally, when the vehicle is decelerating, the electric machine can capture part of the vehicle's kinetic energy and recharge the battery.

A power-split HEV, as known as series/parallel hybrids, often consists of two electric machines and a power-split device, which is referred as an electrical continuously variable transmission (ECVT). As shown in Fig. 1, the engine power can be split into two different power paths. First, similar to a parallel hybrid vehicle, the power-split powertrain has separate engine power-flow path and battery-motor power-flow path (solid lines). Secondly, similar to a series hybrid vehicle, there exists an engine-generator-motor power path. Such a system can be designed to take advantage of both parallel and series hybrids.

The power-split HEV has become increasingly popular over the past ten years. The first production power-split passenger vehicle, the Toyota Hybrid System (THS), was discussed in a paper by Hermance (1999). This system, often known as a single-mode split hybrid, is the heart of Prius and the rest of the hybrid fleet from Toyota currently on the market. Another major design for power-split HEV on the market is the Advanced Hybrid System (Holmes et al., 2003) from General Motors, also known as dual-mode AHS. This system was applied to several full-sized SUVs (Chevy Tahoe and GMC Yukon) and become a major competitor in recent years.

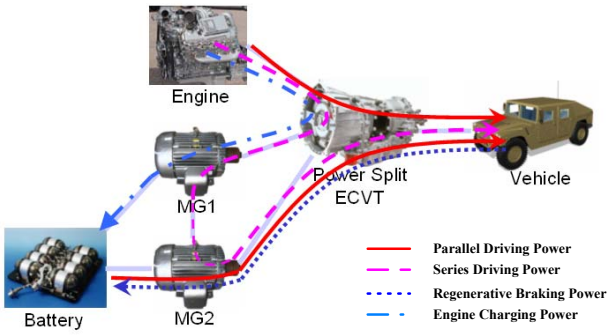

Fig. 1. Example HEV Power flows

In addition to these two popular powertrains, the power-split HEVs can be designed with different engine-to-gear, motor-to-gear, or clutch-to-gear connections. Besides serving the purpose of power transferring, these different gear train configurations allow various kinematic relations between the power components and provide different operating options. Several other configurations can be found in the literature. Some of these designs consist of two planetary gears (Holmes et al., 2003) and others consist of three or more planetary gears (Schmidt, 1999). For a single planetary gear, there are three gear nodes that can be used to link to power sources. More planetary gears provide more flexibility in gear gains and shifting options. With this large number of possible configurations, there are literally thousands of possible options for a power-split vehicle. This provides great freedom for the hybrid vehicle design, but the tasks of exploring and analyzing various powertrain configurations become challenging. It is time consuming for the designer to manually develop models for each configuration and evaluate its performance by simulations. Modelling techniques that enable the designer to bring the configuration design to simulation model accurately and efficiently are desired.

Several studies on the power-split HEV powertrain-system modelling can be found in the literature. Rizoulis et al. (2001) presented a mathematical model of a vehicle with a power-split device based on the steady-state performance. Miller (2006) summarized the models of current power-split HEV

architectures. A comparative analysis of the system efficiency among different power-split configurations was done by Conlon (2005), who used a mathematical model to present the gear split ratios regardless of the powertrain designs. Despite these early efforts, to our knowledge a power-split HEV dynamic model that is flexible enough to cover a wide variety of different designs does not exist in the literature. Such simulation model needs to be flexible enough to accurately describe the powertrain dynamics, and yet simple enough to be used in iterative design process.

In this paper, an automated modelling technique for power-split hybrid powertrains is developed. We first derive the equations for a selected configuration through force analysis. Subsequently, a general form of the dynamic model is derived, based on which an automated generation strategy is introduced. Example configurations are then modelled to demonstrate the process. Applications of such modelling tool are introduced at the end.

2. MODELS OF EXAMPLE POWER-SPLIT HYBRIDS

2.1 Overall Architecture

The selected powertrain configuration is shown in Fig. 2. There are two planetary gear sets (marked as PG1 and PG2). These planetary gear sets, which combine the power and constrain the motions of all the power sources, are the key devices in the split hybrid powertrain. Each planetary gear has three nodes: the sun gear, the carrier gear, and the ring gear. As shown in Fig. 3, several pinion gears connect the three gear nodes to transfer the forces. As a result of the direct mechanical connection through gear teeth, the rotational speed of the ring gear ω_r, sun gear ω_s, and carrier gear ω_c satisfy the following relationship at all times

$$\omega_s S + \omega_r R = \omega_c (R + S) \tag{1}$$

Here R, and S are the radii (or number of teeth) of the ring gear and sun gear, respectively. The lever diagram representation (Benford and Leising, 1981) in Fig. 3 is commonly used to present the speed constraint and simplify the torque analysis for the planetary gear set. The lever diagram presents the rotational speeds of the three gear nodes as vectors rooted at the nodes. Equation (1) then requires that the three speed vectors must form a straight line. The lever diagram is utilized in our study.

It can be seen in Fig. 2 that there are two clutches (marked as CL1 and CL2) in the powertrain system. By locking either clutch CL1 or CL2, ring gear of PG2 can be grounded or locked with the sun gear of PG1 to achieve two operating modes. These two modes are commonly referred to as input split mode (CL1 locked and CL2 released), and compound split mode (CL2 locked and CL1 released) (Holmes et al., 2003). The transients of the clutch release/engagement are ignored. In other words, the mode shift is assumed to occur instantaneously without energy loss.

Besides the connections with the clutches, the ring gear of PG1 connects to the sun gear of PG2. The engine and motor/generator 1 (MG1) are connected to the carrier gear and sun gear of PG1, respectively. The motor/generator 2 (MG2) and output torque to the final drive go through the sun gear and carrier gear of PG2, respectively. The connections above construct the mechanical path of the powertrain. The two electrical machines are also wired with an inverter that is connected to the battery. These components construct the electrical path of the powertrain. Modelling of these two propulsion paths are explained in the following sections.

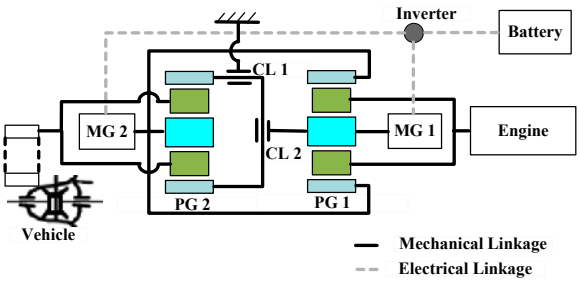

Fig. 2: A Dual-Mode ECVT Hybrid System.

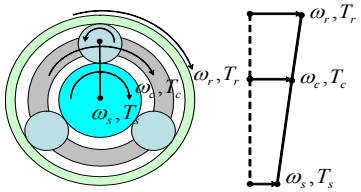

Fig. 3: Planetary gear set and lever diagram.

2.2 Mechanical Power Path Modelling

Fig. 4 shows the free body diagram of the dual-mode powertrain system. The planetary gear sets are represented by two levers. R_1, S_1 and R_2, S_2 represent the ring gear and sun gear radii of the PG1 and PG2, respectively. F_1 and F_2 represent the internal forces between the pinion gears and the sun gears or ring gears. The dynamic models of the two modes are derived separately in the following.

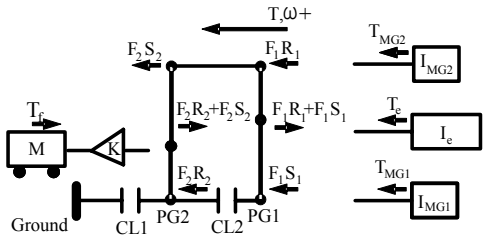

Fig. 4: Free body diagram of the dual-mode powertrain.

In the input-split mode, the CL1 is engaged and CL2 is released. The ring gear of PG2 is thus grounded. The speed constraint on PG2 then becomes

$$\omega_{c2}(R_2 + S_2) = \omega_{r2} S_2 \tag{2}$$

where ω_{c2} and ω_{r2} are the rotational speed of the carrier gear and the ring gear of PG2. The PG1 still satisfies the original speed constraint

$$\omega_{c1}(R_1 + S_1) = \omega_{r1} R_1 + \omega_{s1} S_1 \tag{3}$$

where ω_{c1}, ω_{r1}, and ω_{s1} are the rotational speed of the carrier gear, ring gear, and sun gear of PG1. Apply the Euler equation to study the dynamic system, on the four nodes of the combined lever diagram, we have

$$\dot{\omega}_{MG2}(I_{MG2} + I_{r1} + I_{s2}) = T_{MG2} + F_1 \cdot R_1 + F_2 \cdot S_2 \tag{4}$$

$$\dot{\omega}_e(I_e + I_{c1}) = T_e - F_1 \cdot (R_1 + S_1) \tag{5}$$

$$\dot{\omega}_{MG1}(I_{MG1} + I_{s1}) = T_{MG1} + F_1 \cdot S_1 \tag{6}$$

$$\dot{\omega}_{out}\left(\frac{R_{tire}^2}{K^2}m+I_{c2}\right)=-(F_2R_2+F_2S_2)-\frac{1}{K}\left[T_{fb}-mgf_rR_{tire}-0.5\rho AC_d\left(\frac{\omega_{out}}{K}\right)^2R_{tire}^{\ 3}\right] \quad (7)$$

Equations (4)-(7) can be put into a matrix form with the last two rows presenting the constraints from the two planetary gears. The dynamics of the engine ω_e, electrical machines ω_{MG1} and ω_{MG2}, and vehicle wheel ω_{out} are then governed by

$$\begin{bmatrix}\dot{\omega}_e\\ \dot{\omega}_{out}\\ \dot{\omega}_{MG1}\\ \dot{\omega}_{MG2}\\ F_1\\ F_2\end{bmatrix}=\begin{bmatrix} I_e+I_{c1} & 0 & 0 & 0 & R_1+S_1 & 0\\ 0 & \frac{R_{tire}^2}{K^2}m+I_{c2} & 0 & 0 & 0 & R_2+S_2\\ 0 & 0 & I_{MG1}+I_{s1} & 0 & -S_1 & 0\\ 0 & 0 & 0 & I_{MG2}+I_{r1}+I_{s2} & -R_1 & -S_2\\ R_1+S_1 & 0 & -S_1 & -R_1 & 0 & 0\\ 0 & R_2+S_2 & 0 & -S_2 & 0 & 0\end{bmatrix}^{-1} \quad (8)$$

$$\begin{bmatrix} T_e\\ -\frac{1}{K}\left[T_{fb}+mgf_rR_{tire}+0.5\rho AC_d\left(\frac{\omega_{c2}}{K}\right)^2R_{tire}^{\ 3}\right]\\ T_{MG1}\\ T_{MG2}\\ 0\\ 0\end{bmatrix}$$

In the compound split mode, the clutch CL1 is released and CL2 is locked, forcing the ring gear of PG2 to rotate at the same speed as the sun gear of PG1. Follow a similar procedure, the dynamic equation can be derived as

$$\begin{bmatrix}\dot{\omega}_e\\ \dot{\omega}_{out}\\ \dot{\omega}_{MG1}\\ \dot{\omega}_{MG2}\\ F_1\\ F_2\end{bmatrix}=\begin{bmatrix} I_e+I_{c1} & 0 & 0 & 0 & R_1+S_1 & 0\\ 0 & \frac{R_{tire}^2}{K^2}m+I_{c2} & 0 & 0 & 0 & R_2+S_2\\ 0 & 0 & I_{MG1}+I_{s1}+I_{r2} & 0 & -S_1 & -R_2\\ 0 & 0 & 0 & I_{MG2}+I_{r1}+I_{s2} & -R_1 & -S_2\\ R_1+S_1 & 0 & -S_1 & -R_1 & 0 & 0\\ 0 & R_2+S_2 & -R_2 & -S_2 & 0 & 0\end{bmatrix}^{-1} \quad (9)$$

$$\begin{bmatrix} T_e\\ -\frac{1}{K}\left[T_{fb}+mgf_rR_{tire}+0.5\rho AC_d\left(\frac{\omega_{c2}}{K}\right)^2R_{tire}^{\ 3}\right]\\ T_{MG1}\\ T_{MG2}\\ 0\\ 0\end{bmatrix}$$

Since we ignore the gear shifting dynamics, up-shift and down-shift are treated as nothing but switching between the two modes. Holmes et al. (2003) explained that such dual-mode design allows a "stepless" shift between the two driving modes so that it minimizes the torque lost during the shift. Based on this concept, when the controller commands to switch clutches, simulation outputs are switched from one model to the other.

2.3 Electrical Power Path Modelling

The power requirements from the two motor/generators are supplied by the power storage device (battery), and can be calculated from the equation

$$P_{batt}=(T_{MG1}\omega_{MG1}\eta_{MG1}^{\ k}+T_{MG2}\omega_{MG2}\eta_{MG2}^{\ k})\eta_i \ , \quad (10)$$

where η_{MG1} and η_{MG2} are the efficiency of the electric machines. The exponential k is the sign of the power flow direction. k=-1 when the battery is discharged and k=1 when it is charged. η_i represents the efficiency of the inverter.

For simplicity, the internal resistance model (see Fig. 5) is used to represent the battery performance. The open circuit voltage V_{oc} and resistance R_{batt} are both state-dependent parameters. They are functions of the battery state of charge (SOC) and temperature. The battery temperature is assumed to be constant (20 °C) and its effects are ignored. The dependency on SOC is represented in lookup tables.

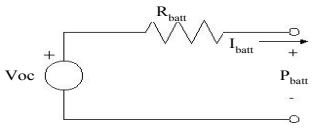

Fig. 5: Internal resistance battery model.

SOC reflects the battery energy status and is a key state variable. Its rate of change depends on the equivalent battery capacity Q_{max} and the current I_{batt}:

$$\dot{SOC}=-\frac{I_{batt}}{Q_{\max}} \quad (11)$$

The battery capacity Q_{batt} is a function of temperature, and is approximated as a constant value in this paper. Battery current I_{batt} is a function of V_{oc} and R_{batt}, which relate to the battery power output as

$$P_{batt}=V_{oc}I_{batt}-I_{batt}^2R_{batt} \quad (12)$$

Solve the equations (10)-(12),

$$\dot{SOC}=-\frac{V_{oc}-\sqrt{V_{oc}^{\ 2}-4(T_{MG1}\omega_{MG1}\eta_{MG1}^{\ k}+T_{MG2}\omega_{MG2}\eta_{MG2}^{\ k})\eta_iR_{batt}}}{2R_{batt}Q_{\max}} \quad (13)$$

Equation (13) directly links the torque variables of the two electric machines to the rate of change of battery state of charge. This equation together with (8) and (9), describe the dynamics of this dual-mode power-split vehicle.

3. AUTOMATED MODELING OF POWER-SPLIT HYBRID SYSTEMS

3.1 Universal Format of the Dynamic Model

The model development process, as presented in the previous section, is straightforward but tedious. Mistakes could happen in the hand derivation of dynamic models, including erroneous signs or gear teeth numbers. This section introduces a universal format of the dynamic model, which enables an automated modelling process for different configurations.

Let's revisit equation (8). The coefficient matrix is symmetric and can be divided into four sub-matrices with J denoting the upper-left 4×4 inertia matrix and D representing the up-right 4×2 matrix that shows the gear train constraints. Because the torques on each node remain proportional to the corresponding coefficients in D, for each constraint i, it can define a Lagrange multiplier λ_i (Hibbeler and Fan, 1997), which indicates how strongly the constraint must push the associated inertias to maintain the correct velocities. And it is easy to see that the λ_i is equal to the internal forces F_i. And these constraints appear in dual forms of D and D^T, where D relates the coefficient with internal forces and D^T relates the node speeds. Equation (8) can then be represented as

$$\begin{bmatrix}\dot{\Omega}\\ F\end{bmatrix}=\begin{bmatrix}J & D\\ D^T & 0\end{bmatrix}^{-1}\begin{bmatrix}T\\ 0\end{bmatrix} \ , \quad (14)$$

where □ and T are the speed and torque vectors of the four nodes. Note that the battery dynamics in equation (13) is independent of the powertrain configuration and thus does not change. Only the mechanical part of the model varies with the configuration. The significance of (14) is the fact that the speeds of the nodes can be simulated directly from the node torques. In other words, after the topology of the

powertrain system is specified, the model of the system can be generated automatically. This process is summarized in the following section.

3.2 Automated Model Development

The dynamic model built in this process makes the following assumptions. Only the vehicle longitudinal dynamics are considered; the mechanical efficiency of the gear trains are high and the loss is neglected; The clutch engagement dynamics (if a clutch exists in the system) are ignored and the synchronizing shifting operation between different mode is achieved by switching between different models (Holmes et al, 2003); The studied powertrain configuration only consists of one engine, two MGs, and one vehicle output shaft.

Step 1: Determine the kinematical constraint matrix D

Based on the powertrain configuration, one can apply the following rules to obtain a kinematical constraint matrix *D*.

Rule 1: The number of columns in *D* is equal to the number of planetary gears.

Rule 2: The number of rows in *D* is equal to the number of columns in *D* plus two, each representing a node on the lever diagram.

Rule 3: For the power source component(s) at each row, a "node coefficient" should be entered. The "node coefficient" is equal to: *-Si* if connected to the sun gear; *-Ri* if connected to the ring gear; and *Ri+Si* if connected to the carrier gear. Here the subscript *i* represents the *i*th planetary gear set.

Rule 4: Fill all other entries in matrix *D* with zeros.

Rule 5: For 3 or more PGs system, after the original matrix *D* is obtained. It can be further simplified to a 4×2 matrix (one output, one engine, and two MGs will form no more than 4 nodes). This is done by using the kinematic relations from the free-rolling node(s) that is not connected to any power source or vehicle.

Step 2: Determine the inertia matrix J

Matrix *J* is a diagonal square matrix. The entry of each diagonal term is the inertia of each node. The node inertia is equal to the inertia of the power components. The inertias are I_e for the engine, I_{MG} for electric machines, and mR_{tire}^2/K^2 for the vehicle. Because the gear inertias are much smaller compared with the power sources and the vehicle, they can be ignored. Assume a convention that the first row of both matrix *J* and matrix *D* represents the engine node, the second row represents the output node connected to the vehicle, the third row represents the MG1 node, and the fourth row represents the MG2 node. The matrix *J* then has the format

$$J = \begin{bmatrix} I_e & 0 & 0 & 0 \\ 0 & mR_{tire}^2/K^2 & 0 & 0 \\ 0 & 0 & I_{MG1} & \\ 0 & 0 & 0 & I_{MG2} \end{bmatrix}. \quad (15)$$

Step 3: Finalize the dynamic model

After the matrices *D* and *J* are specified, the dynamic model can be constructed by using (14). In equation (14), Ω consists of the speed of engine ω_e, output shaft ω_{out} (proportional to the vehicle wheel speed ω_{wh} by a factor of final drive ratio *1/K*), and electrical machine(s) ω_{MG}. *T* consists of the node torques applied at nodes corresponding to the respective Ω elements. For the output shaft, driving resistance torque from the vehicle $-\frac{1}{K}\left[T_{fb} + mgf_r R_{tire} + 0.5\rho AC_d(\frac{\omega_{out}}{K})^2 R_{tire}^3\right]$ needs to be included. Finally, in addition to the mechanical path model, the electrical path model is generated in (13), with this completes the dynamic model of the whole powertrain.

4. AUTOMATED MODELING DEMOSTRATIONS

4.1 Model of the Toyota Hybrid System

The Toyota Hybrid System (THS), or sometimes known as the Synergy Drive, is the first commercial vehicle with a power-split hybrid design. A detailed description of its configuration can be found in (Hermance, 1999). As shown in Fig. 6, there is a single planetary gear set. The sun gear (S) connects to MG1, the carrier gear (C) connects to engine, and the ring gear (R) connects to MG2 and the vehicle through a gear ratio *K*.

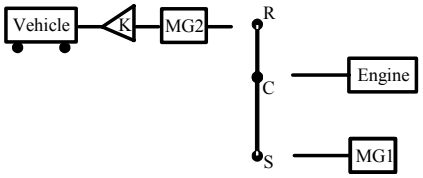

Fig. 6: The powertrain of a single planetary gear system (THS).

Following the rules outlined in the previous section, the matrix D is a 3x1 matrix, with the three nodes defined for the carrier gear, ring gear, and sun gear respectively. For a single planetary gear system, the matrix has one column and three rows. As a convention, we start from the node with engine, vehicle, and then electrical machine(s). The engine is connected to the carrier gear node so that R_1+S_1 is entered into the element in the first row. The vehicle and the MG2, as in the second row, together connect to the ring gear. As a result, the coefficient $-R_1$ is entered into the second row. Similarly, $-S_1$ is entered into the third row for MG1. This completes the matrix *D* as

$$D = \begin{bmatrix} R_1 + S_1 \\ -R_1 \\ -S_1 \end{bmatrix}. \quad (16)$$

Matrix *J* is then generated with the engine, vehicle and MG2, and MG1 as the orders in the rows. And the dynamic model can be finished by using the computer to process.

For the purpose of model validation, this model is put under the command of a rule-based control strategy. In the simulation, vehicle parameters, engine maps and efficiency torque and fuel consumption tables are obtained from ADVISOR 2002. Fig. 7 compares the simulation results with the experiment results from (Duoba et al., 2001). Since we do not know the control gains precisely, and considering all the simplifying assumptions we made, the behaviour of this model was found to agree with the actual system quite well. The rule-based control in this simulation was explained in details in our earlier publication (Liu et al., 2005).

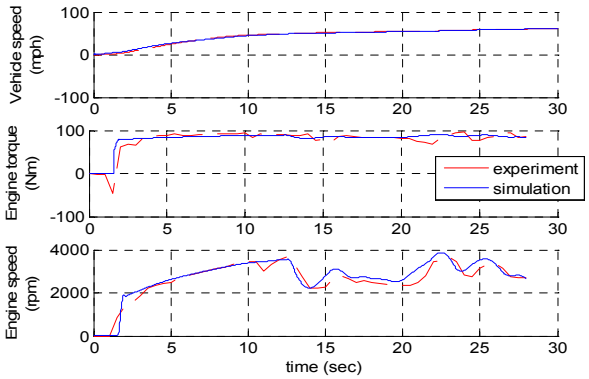

Fig. 7: THS Engine simulation results compared with published experiment results under the same driving cycle.

4.2 Model of a triple planetary gear powertrain

In this example, a three planetary gear (PG) powertrain (Schmidt, 1999) is selected to study the case with a free-rolling node. The additional PG brings the powertrain system one more free node, therefore, the matrix D is now a 5×3 matrix with the five rows correspond to the five nodes and three columns correspond to the three PGs. Except the one node connected to the vehicle final drive, there are apparently four nodes left that can be hooked up with engine and MGs. If two MGs and one engine are selected for the power sources, there is one node left without connecting to anything. This node is the free-rolling node. As a convention, the first row of matrix D is the node with engine, the second is the node with vehicle, the third and fourth are nodes with MGs, and the fifth row is the free-rolling node.

Fig. 8 shows the powertrain of this 3-PG powertrain system. In the input-split speed mode, CL1 is locked and CL2 is released. The engine is connected to the ring gear of the PG1, therefore, a node coefficient $-R_1$ is entered into element (1,1). The vehicle final drive is connected to the carrier gear of the PG3, therefore, R_3+S_3 is entered into element (2,3). MG1 is connected to both ring gear of the PG2 and sun gear of the PG1, therefore, $-S_1$ is entered into element (3,1) and $-R_2$ is entered into element (3,2). MG2 is connected to both sun gears of the PG2 and PG3, therefore, $-S_2$ is entered into element (4,2) and $-S_3$ is entered into element (4,3).

The fifth row of matrix D corresponds to the node/shaft of both carrier gears of the PG1 and PG2 where there is no power source connected. The corresponding node coefficients, in this case, R_1+S_1 is entered into element (5,1) and R_2+S_2 is entered into element (5,2). After filling the rest of the entries with zeros, the matrix D becomes

$$D_{model} = \begin{bmatrix} -R_1 & 0 & 0 \\ 0 & 0 & R_3+S_3 \\ -S_1 & -R_2 & 0 \\ 0 & -S_2 & -S_3 \\ R_1+S_1 & R_2+S_2 & 0 \end{bmatrix} \quad (17)$$

Following rule 5, this originally derived matrix D can be further simplified to a 4×2 matrix D to construct the dynamic model. In (17), the fifth row corresponds to the free-rolling node that is not connected to any power sources. Because the gear inertia on this node is ignored, the dynamics are

$$(R_1+S_1)F_1+(R_2+S_2)F_2=0 \quad (18)$$

From (18),

$$F_2 = -\frac{(R_1+S_1)}{(R_2+S_2)}F_1 \quad (19)$$

Because in matrix D mode1, the first and second columns consist of the node coefficients that multiply with F_1 and F_2, respectively, relationship between these two forces in (19) can then be substituted to simplify the matrix D mode1 as

$$\bar{D}_{model} = \begin{bmatrix} -R_1 & 0 \\ 0 & R_3+S_3 \\ -S_1+\frac{R_1+S_1}{R_2+S_2}R_2 & 0 \\ \frac{R_1+S_1}{R_2+S_2}S_2 & -S_3 \end{bmatrix} \quad (20)$$

The matrix J represents the power source inertia on each node and has the same format as (15). This example demonstrates the process of modelling a triple PG powertrain system. The extra free-rolling node is used to calculate the relationship between the internal forces and the derived relationship simplifies the matrix D to a 4×2 matrix.

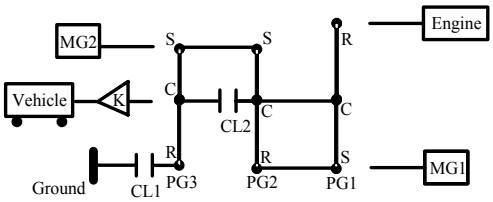

Fig. 8: The powertrain of the triple planetary gear system of (Schmidt, 1999).

5. APPLICATIONS OF THE AUTOMATED MODEL

The proposed math-based model generation process provides a one-to-one correspondence between the powertrain configuration and the model matrix. On one hand, given a configuration design, the corresponding kinematic matrix D can be derived using the rules presented above. On the other hand, given a matrix D, the corresponding configuration is uniquely defined. For example, for the D matrix given in Eq.(21), the corresponding powertrain configuration can be derived as follows. The R_1+S_1 at the (1,1) element indicates that the engine connects to the carrier gear of PG1; $-R_1$ and R_2+S_2 at the (2,1) and (2,2) elements indicate that the output shaft connects to both the ring gear of PG1 and the carrier gear of PG2; $-S_1$ at the (3,1) element indicates the connection between MG1 and the sun gear of PG1; and $-R_2$ at the (4,2) element indicates the connection between MG2 and the ring gear of PG2. The absence of $-S_2$ in the second column indicates that the sun gear of PG2 is grounded. As a result, the corresponding configuration can be drawn in Fig. 9.

$$D = \begin{bmatrix} R_1+S_1 & 0 \\ -R_1 & R_2+S_2 \\ -S_1 & 0 \\ 0 & -R_2 \end{bmatrix} \quad (21)$$

The fact that there is a one-to-one relationship between the matrix D and the configuration design makes it possible to identify all possible configuration designs. For example, to construct a 2-PG powertrain system, the process of enumerating all possible solutions is as follows. The matrix J

of the desired 2-PG powertrain is fixed as shown in (15) for all different configurations assuming the gear inertia can be ignored. The matrix D of the desired 2-PG powertrain is a 4×2 matrix with the two columns representing the two PGs. In each column, a power-split PG (the three nodes are all connected to either power sources or vehicle output) has one zero and three node coefficients while a power-ratio PG (one of the three PG nodes is locked to the ground by a clutch and the other two nodes are connected to either power sources or vehicle output) has two zeros and any two of the three node coefficients. Apparently for a single column in a matrix D, there could be 24 different combinations for a power-split PG (4!=24), and there could be 36 different combinations for a power-ratio PG (3×(4×3)=36). A valid power-split configuration must consist of at least one power-split PG. And changing the order of the two columns in the matrix D does not change the configuration. Therefore, the total design combinations can be calculated as

$$24 \times 24/2 + 24 \times 36 = 1152 \tag{22}$$

where the first term represents the number of combinations with two power-split PGs and the second term is the number of combinations with one power-ratio PG and one power-split PG. There are 1152 different mathematical combinations in total for a 2-PG power-split powertrain. This represents all mathematically possible designs of a 2-PG system.

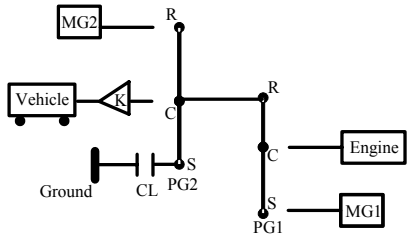

Fig. 9: Constructed configuration based on (21).

Matrix D can be used to calculate the mechanical points of a powertrain system, which are defined as the input/output speed ratios where one of the electric machines has zero speed. The design of the mechanical point (MP) is very critical (Conlon, 2005, Grewe et al., 2007). In matrix D, the first and second rows correspond to the speeds of the input and output nodes, respectively; while the third and fourth rows correspond to the speeds of the two MGs. Therefore, matrix D can be further divided into two sub-matrices

$$D = \begin{bmatrix} D_{11} & \cdots \\ D_{21} & \cdots \\ D_{31} & \cdots \\ D_{41} & \cdots \end{bmatrix} = \begin{bmatrix} D_{EV} \\ D_{MG} \end{bmatrix} \tag{23}$$

where D_{EV} is the first two rows of matrix D and D_{MG} is the third and fourth rows. Substitute this new format of D into the original dynamic equation (14),

$$D^T \dot{\Omega} = D_{EV}^T \begin{bmatrix} \dot{\omega}_e \\ \dot{\omega}_{out} \end{bmatrix} + D_{MG}^T \begin{bmatrix} \dot{\omega}_{MG1} \\ \dot{\omega}_{MG2} \end{bmatrix} = 0 \tag{24}$$

which can be further derived to

$$\begin{bmatrix} \omega_{MG1} \\ \omega_{MG2} \end{bmatrix} = -D_{MG}^{-T} D_{EV}^T \begin{bmatrix} \omega_e \\ \omega_{out} \end{bmatrix} \tag{25}$$

In (25), let either ω_{MG1} or ω_{MG2} equal to zero, the input/output speed ratio between ω_e and ω_{out}, which is the corresponding mechanical point, can be calculated.

6. CONCLUSION

An automated modelling methodology is presented for split-hybrid vehicles. Firstly, one particular powertrain is selected to be modelled through force analysis. Subsequently, a general dynamic model is proposed and a model generation strategy is introduced. Three examples are discussed to demonstrate this modelling process. Finally, possible applications of this modelling process are suggested.

ACKNOWLEDGEMENTS

This work is supported by the Automotive Research Center of the University of Michigan, a Center of Excellence sponsored by the U.S. Army TARDEC under the contract DAAE07-98-C-R-L008.

REFERENCE

Benford, H.L. and Leising, M.B., (1981), The Lever Analogy: A New Tool in Transmission Analysis, *SAE* 810102.

Conlon, B., (2005), Comparative Analysis of Single and Combined Hybrid Electrically Variable Transmission Operating Modes, *SAE* 2005-01-1162.

Duoba, M., Ng, H., and Larsen, R., (2001), Characterization and Comparison of Two Hybrid Electric Vehicles (HEVs) – Honda Insight and Toyota Prius, *SAE* 2001-01-1335.

Evans, D.G., Polom, M.E., Poulos, S.G., Maanen, K., Zarger, T.H., (2003), Powertrain Architecture and Controls Integration for GM's Hybrid Full-Size Pickup Truck, *SAE* 2003-01-0085.

Grewe, T.M., Conlon, B.M., Holmes, A.G., (2007), Defining the General Motors 2-Mode Hybrid Transmission, *SAE* 2007-01-0273.

Hermance, D., (1999), Toyota Hybrid System, *1999 SAE TOPTEC Conference*, Albany, NY, May 1999.

Hibbeler, R.C. and Fan, S.C., *Engineering mechanics: dynamics*, Prentice Hall, 1997.

Holmes, A.G., Klemen, D., Schmidt, M.R., (2003), Electrically Variable Transmission with Selective Input Split, Compound Split, Neutral and Reverse Modes, *US Patent* 6,527,658 B2, issued Mar. 4, 2003

Liu, J., Peng, H., Filipi, Z., (2005), Modeling and Control Analysis of Toyota Hybrid System, *International Conference on AIM*, Monterey, CA. Jul. 24-28, 2005.

Miller, J.M., (2006), Hybrid Electric Vehicle Propulsion System Architectures of the e-CVT Type, *IEEE Transactions on Power Electronics*, Vol.21, No. 3, pp 756-767, May 2006.

Rizoulis, D., Burl, J., and Beard, J., (2001), Control Strategies for a Series-Parallel Hybrid Electric Vehicle, *SAE* 2001-01-1354.

Schmidt, M.R., (1999), Two-Mode, Compound-Split Power, Electro-Mechanical Vehicular Transmission, *US Patent* 5,931,757, Issued Aug. 1999.